

Title	Ru passivated and Ru doped e-TaN surfaces as combined barrier and liner material for copper interconnects: a first principles study
Authors	Kondati Natarajan, Suresh;Nies, Cara-Lena;Nolan, Michael
Publication date	2019-05-21
Original Citation	Kondati Natarajan, S., Nies, C.-L. and Nolan, M. (2019) 'Ru passivated and Ru doped e-TaN surfaces as combined barrier and liner material for copper interconnects: a first principles study', Journal of Materials Chemistry C, 7(26), pp. 7959-7973. doi: 10.1039/C8TC06118A
Type of publication	Article (peer-reviewed)
Link to publisher's version	10.1039/C8TC06118A
Rights	© 2019, the Authors. Published by the Royal Society of Chemistry. All rights reserved.
Download date	2024-04-24 09:10:05
Item downloaded from	https://hdl.handle.net/10468/8212

Electronic Supplementary information for "Ru Passivated and Ru Doped ϵ -TaN surfaces as Combined Barrier and Liner Material for Copper Interconnects: A First Principles Study"

Suresh Kondati Natarajan*, Cara-Lena Nies* and Michael Nolan

S1: TaN phase diagram

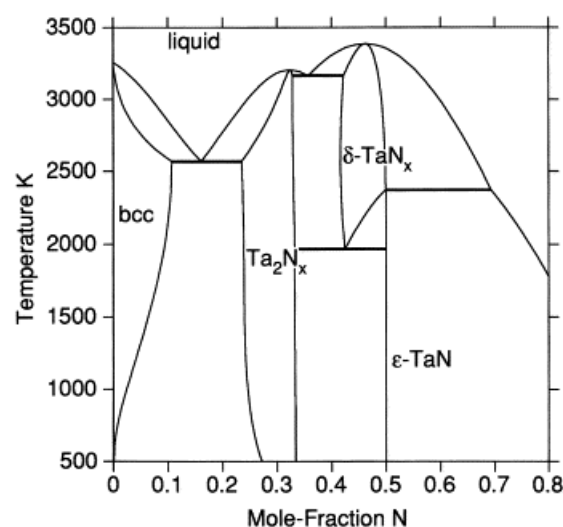


Figure S1: TaN phase diagram [Frisk(1998)]. Licence no. to reuse figure: 4481420260380

S2: ϵ -TaN low index surfaces

Table S1 lists the essential geometric properties and surface energies of the low index surfaces. Figure S2 shows the geometries of all ($2^3-1 = 7$) low index surfaces of ϵ -TaN. Here, the geometries of (0 1 0) and (1 0 0) surfaces are symmetrically identical, so are the geometries of (1 0 1) and (0 1 1). The surfaces (1 1 0), (1 1 1) and (1 0 0) are the three lowest energy surfaces and thus these surfaces are considered for detailed analysis in the main text.

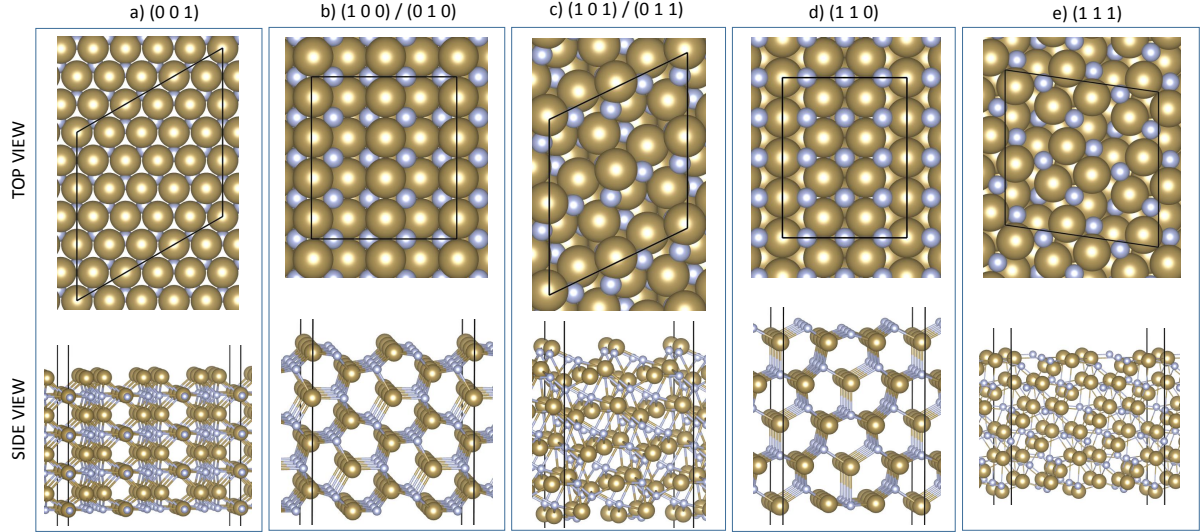


Figure S2: All low index surfaces of ϵ -TaN

Table S1: Details of the computation model of the low index surfaces of ϵ -TaN.

Surface	Supercell	K-points	Surf. Area [nm ²]	Layers	TaN/layer	Slab Thickness [Å]	No. Atoms	E _{Surf} [J/m ²]
(0 0 1)	(3×3)	1×1×1	2.1	4	27	10.0	216	3.3
(1 0 0)/(0 1 0)	(1×4)	2×2×1	1.2	8	8	10.2	128	2.7
(1 0 1)/(0 1 1)	(2×2)	2×2×1	1.1	5	12	11.4	120	3.4
(1 1 0)	(1×4)	3×2×1	1.1	5	12	11.8	120	2.6
(1 1 1)	(2×2)	3×3×1	1.4	6	12	10.5	144	2.7

S3: Bulk Ru, Ru (0 0 1) surface and Cu on Ru(0 0 1) surface

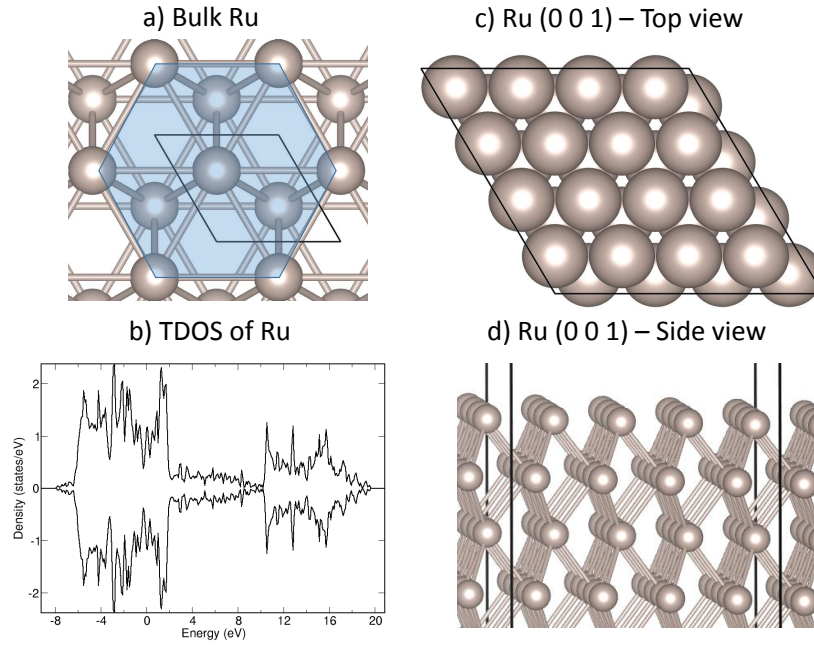


Figure S3: Panel a) shows the bulk geometry of Ru metal (brown spheres) in HCP lattice where the unit cell is marked by solid black lines and the blue shaded region represents the hexagonal symmetry. Total DOS of bulk Ru showing metallic character is given in panel b). Top and side views of Ru(0 0 1) surface are shown in panels c) and d), respectively.

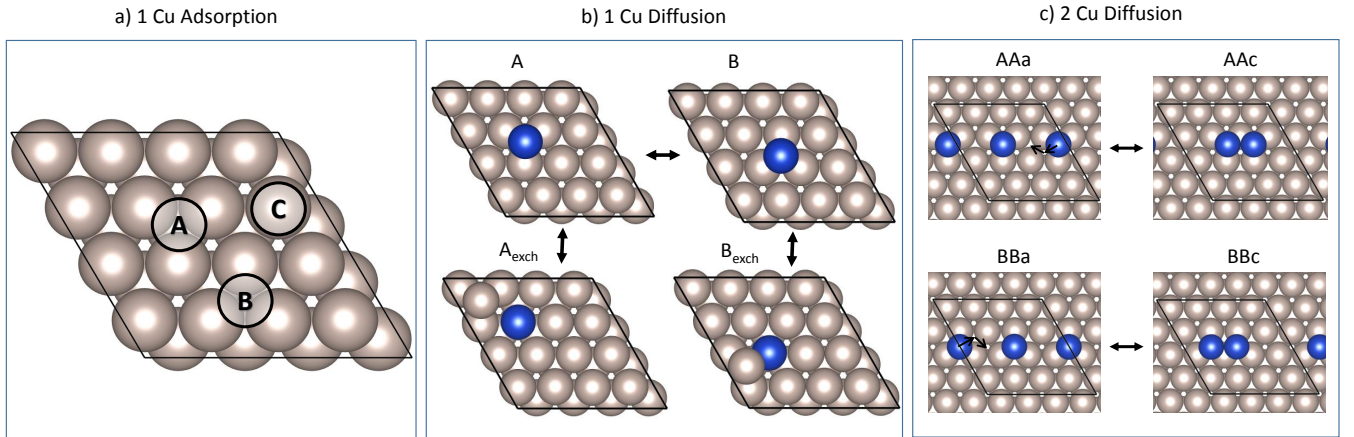


Figure S4: Panel a) shows stable binding sites for Cu adatoms at the (0 0 1) surface of Ru. Endpoints (minima) used to compute the activation energies for the facile as well as sub-surface diffusion of one Cu adatom on the Ru(0 0 1) surface are shown in panel b) and the endpoints for the facile diffusion of two Cu adatoms are shown in panel c). The Ru and Cu atoms are shown in brown and blue, respectively.

S4: Cu/Ru on TaN surfaces

S4.1: 1 Cu/Ru on TaN

On the (1 1 0) surface, five other stable sites B, C, D, E and F with relatively lower binding energies are also identified. Site B is a 4-fold site coordinated by 2 N and 2 Ta atoms, while C is atop N site coordinated by 4 surface Ta atoms, D is atop Ta site, E is atop N site coordinated by 3 surface Ta atoms and F is another 4-fold site coordinated by 2 Ta and 2 N atoms. The binding energies are in the range of -1.92 eV to -2.81 eV for Cu and -3.68 eV to -4.95 eV for Ru. The least preferable adsorption site for Cu adatom is the site C, and site B is the least favourable for Ru adsorption. Ru adatom was unstable at sites C, D and E. At all the sites the Ru-Ta distances are shorter than the Cu-Ta distances, whereas the Ru-N and Cu-N distances are almost the same. From the Bader charge analysis we find that both Cu and Ru adatoms are oxidized with average Bader charges of 0.53 and 0.21 $|e|$ (see Table S2) at this surface as expected due to the electron affinity differences between Cu/Ru and Ta/N. The electron affinity values of Cu, Ru, Ta and N are 1.235, 1.046, 0.32 and -0.07, respectively. An in-depth analysis of the surface valence charges for Cu/Ru binding at site A is given in section S5 of the ESI. In addition to that, the PDOS plots of the Cu and Ru adatoms at the most favourable sites on the low-index surfaces of TaN are discussed in section S6 of the ESI.

On the (1 1 1) surface there are two unique stable sites A and B, where A is a two fold bridge site and B is a wide hollow site between a pair of N and Ta atoms. Site B is more favoured (about 0.4 - 0.5 eV) than site A by both Ru and Cu adatoms. Similar to the (1 1 0) surface, we find that the Ru adatom binds at least 2 eV stronger than the Cu adatom. In contrast to the (1 1 0) surface we find that both Cu and Ru adatoms are reduced, Ru more so than Cu (see Table S2). Reduction is most prominent at site A for both Ru and Cu adatoms where the surface N atoms are farther from them than the surface Ta atoms. At site B, where the N atoms are moderately closer to the adatoms, we find a considerably decreased charge gain by the adatoms. This indicates that the adatoms gain electrons from the neighbouring Ta atoms, which are not as oxidized as those in the (1 1 0) surface. Ta atoms also have a larger electron affinity than N.

On the (1 0 0) surface there are three stable sites A, B and C, where site A is along the surface trench coordinated by 2 Ta and 1 N atoms, B is a three fold site made by 2 Ta and 1 N atoms and C is a two fold bridge site coordinated by 2 Ta atoms. Moreover, site C is present along the pathway connecting sites A and B. The Cu adatom binds with almost the same binding energy at sites A and C, with A being the most favourable for both Ru and Cu, but does not bind at site B as it relaxes to site C, however, Ru binds to site B as well. Similar to the (1 1 1) surface, the Cu and Ru adatoms are reduced to some degree at this surface as evident from the valence charges reported in Table S2.

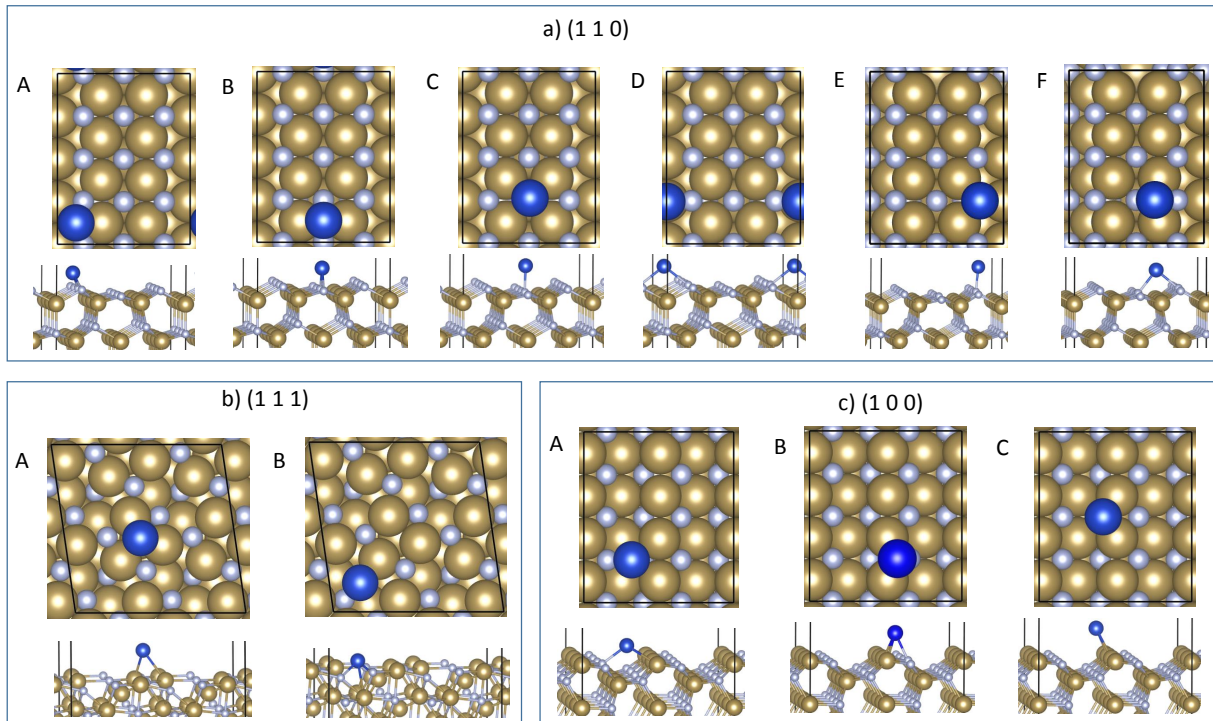


Figure S5: Panels a), b) and c) shows the top and perspective side views of the Cu/Ru adatoms at unique stable binding sites on the (1 1 0), (1 1 1) and (1 0 0) surfaces of ϵ -TaN, respectively. The Ta and N atoms are shown in ochre and light blue, respectively. The adatom (Cu or Ru) is shown in blue.

Table S2: Average distances, valence electronic charge and binding energies of Cu and Ru adatoms on the low index surfaces of ϵ -TaN along with activation energies involved in the inter-minimum hopping of the adsorbed Cu and Ru adatoms. $d(X-Y)$ gives the average bond distance between the neighbouring X and Y species in the corresponding minimum geometries. $Q(X)$ gives the average valence electronic charge of atom X according to the Bader charge partitioning scheme. The '=' sign indicates that the activation energy is the same for both forward and reverse hops. (') next to A or B indicates that it is a symmetry equivalent site along the trench at the surface, while a (") refers to a symmetry equivalent site across the trench as shown in Figure 3 in main text.

Surface	Sites	Interatomic distance [Å]						Q(Cu)	Q(Ru)	E _{bind} [eV/ads.]		Pathway	E _{activation} [eV]	
		Cu-Cu	Ru-Ru	Cu-N	Ru-N	Cu-Ta	Ru-Ta			Cu	Ru		Cu	Ru
1 Cu/Ru adatom														
(1 1 0)	A			1.9	1.9	2.8	2.6	10.5	7.8	-2.82	-4.95	A=A'	0.69	1.49
	B			2.1	2.0	2.6	2.6	10.5	7.6	-2.04	-3.68	B=B'	0.13	0.98
	C			1.8	-	3.2	-	10.5	-	-1.92	-	A-B	1.37	2.09
	D			2.1	-	2.4	-	10.4	-	-2.13	-	B-A	0.59	0.82
	E			1.8	-	2.6	-	10.5	-	-2.12	-			
	F			2.0	1.9	2.7	2.6	10.4	7.6	-2.25	-3.85			
(1 1 1)	A			3.2	2.8	2.6	2.4	11.4	8.7	-2.80	-5.15	A-B	0.85	1.88
	B			2.0	2.0	2.5	2.4	11.2	8.4	-3.21	-5.64	B-A	1.26	2.37
(1 0 0)	A			2.1	2.1	2.7	2.6	11.1	8.3	-3.26	-5.67	A=A'	0.50	0.68
	B			-	2.1	-	2.4	-	8.3	-	-5.37	A-C	0.12	0.36
	C			3.1	3.1	2.6	2.4	11.2	8.5	-3.22	-5.34	C-A	0.08	0.03
												C-B	-	0.23
												B-C	-	0.25
												C-A''	1.04	-
												A''-C	1.08	-
												B-A''	-	0.92
												A''-B	-	1.23

S4.2: 2 Cu/Ru on TaN

On the (1 1 0) surface, the first adatom is placed at site A and the other adatom is placed at one of the following sites: B (AB), C (AC), D (AD), E (AE), F (AF), A'' (AA''), on top of the adatom at site A (AA-top), A' adjacent to A (AA'c) and A' away from A (AA'a). The binding energies per adatom are in the range of -2.41 eV to -2.98 eV for Cu and -4.14 eV to -5.04 eV for Ru. Comparing the above results to the 1 adatom case, we do not find a significant increase in the binding energies per Cu atom even though the two adatoms are close to each other in several minimum geometries. Therefore the adatom-adatom interaction must be very low. The most favourable binding is observed when the Cu or Ru atoms are adsorbed at sites A and A'' (AA'') which are located adjacent to each other on the (1×4) supercell of TaN (1 1 0) surface and the least favourable binding is observed when the Ru adatoms are adsorbed on top of one another at site A (AA-top) and when Cu adatoms are adsorbed at sites A and B. Similar to the 1 adatom case, the Ru and Cu adatoms are oxidized at all sites on this surface

On the (1 1 1) surface, another geometry is considered where the two adatoms are placed on top of each other at site B (BB-top), however, this geometry is found to be unstable for both Cu and Ru adatoms and reverted to A2B. The associated state (B2A) is found to be unstable in the case of Cu adatoms.

On the (1 0 0) surface the first adatom is placed at site A and the other adatom is placed at the following sites: B (AB), C (AC), on top of the adatom at site A (AA-top), A' close to A (AA'c) and A' away from A (AA'a). The binding energies per adatom are in the range of -3.00 eV to -3.37 eV for Cu and -5.18 eV to -5.74 eV for Ru. Vertically stacked Cu/Ru adatoms at site A (AA-top) are found to be unstable and relaxed to AC. The associated state AA'c is the most favourable 2 atom site for Cu adatoms whereas the separated state AA'a is the most favourable for Ru adatoms. The Cu adatom remains metallic at site A and reduced at site C while the Ru adatom shows mild reduction at all sites.

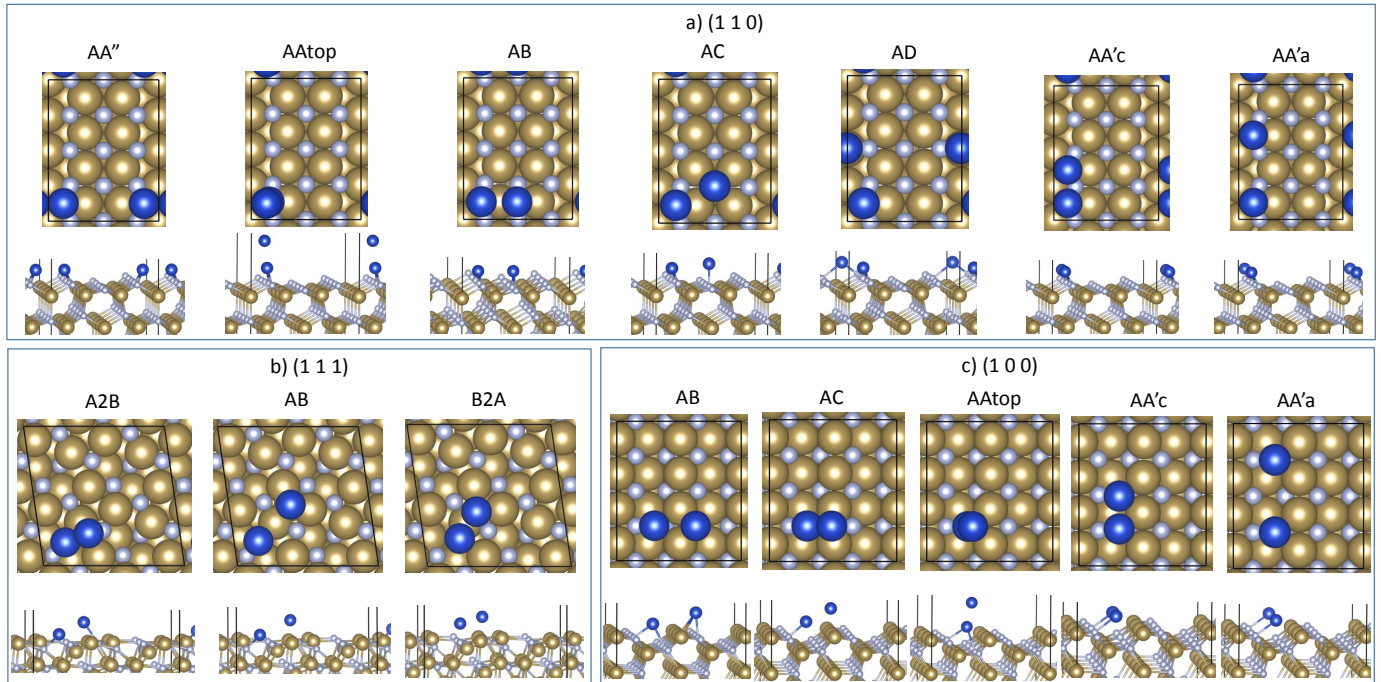


Figure S6: Geometries of 2 adatoms (Cu/Ru) at the unique 2 atom binding sites at the low index surfaces of ϵ -TaN. Here A2B represents the geometry where the adatom at A moved towards the adatom at site B and vice-versa. AA'c and AA'a represents 2 atom sites where the adatoms are close to each other and distant from each other, respectively. The Ta and N atoms are shown in ochre and light blue, respectively. The adatom (Cu or Ru) is shown in blue.

Table S3: Average distances, valence electronic charge and binding energies of Cu and Ru adatoms on the low index surfaces of ϵ -TaN along with activation energies involved in the inter-minimum hopping of the adsorbed Cu and Ru adatoms. $d(X-Y)$ gives the average bond distance between the neighbouring X and Y species in the corresponding minimum geometries. $Q(X)$ gives the average valence electronic charge of atom X according to the Bader charge partitioning scheme. The '=' sign indicates that the activation energy is the same for both forward and reverse hops. (') next to A or B indicates that it is a symmetry equivalent site along the trench at the surface, while a (") refers to a symmetry equivalent site across the trench as shown in Figure 3 in main text.

Surface	Sites	Interatomic distance [Å]						Q(Cu)		Q(Ru)	E _{bind}	[eV/ads.]		Pathway	E _{activation} [eV]	
		Cu-Cu	Ru-Ru	Cu-N	Ru-N	Cu-Ta	Ru-Ta	Cu	Ru	Cu	Ru	Cu	Ru			
(1 1 0)		2 Cu/Ru adatom														
	AB	2.9	2.4	2.0	2.0	2.8	2.9	10.5/10.5	7.6/7.5	-2.41	-4.50					
	AC	-	-	-	-	-	-	-	-	-	-					
	AD	4.6	-	2.0	-	2.7	-	10.5/10.5	-	-2.42	-					
	AE	-	-	-	-	-	-	-	-	-	-4.79					
	AF	4.7		1.9		2.8		10.5/10.5	7.8/7.6	-2.45	-4.31					
	AA''	2.4	2.4	2.0	2.0	2.8	2.8	10.6/10.6	7.7/7.5	-2.98	-5.04					
	AA'-top		2.1		2.8		3.7		7.6/7.9	-	-4.14					
(1 1 1)	AA'c	2.9	2.9	2.0	2.0	2.9	2.8	10.5/10.5	7.9/7.7	-2.70	-4.95		AA'a-AA'c	0.73	1.32	
	AA'a	5.8	5.8	1.9	1.9	2.8	2.7	10.5/10.5	7.7/7.7	-2.77	-4.81		AA'c-AA'a	0.57	1.60	
	AB	3.8	4.0	2.5	2.6	2.6	2.4	11.2/11.3	8.4/8.7	-3.04	-5.37		AB-A2B	0.20	0.16	
	BB-top	-	-	-	-	-	-	-	-	-	-		A2B-AB	0.06	0.47	
	B2A	-	2.6	-	2.9	-	2.4	-	8.5/8.6	-	-4.94		AB-B2A	-	0.93	
	A2B	2.4	2.4	2.0	2.0	2.7	2.6	11.0/11.1	8.3/8.2	-2.96	-5.53		B2A-AB	-	0.07	
	(1 0 0)	AB	-	2.8	-	2.1	-	2.6	-	8.2/8.1	-	-5.18				
		AC	2.3	2.4	2.7	2.6	2.8	2.9	10.8/11.2	8.0/8.6	-3.00	-5.47				
AA-top		-	-	-	-	-	-	-	-	-	-					
AA'c		2.7	3.0	2.1	2.0	2.7	2.7	11.0/11.1	8.3/8.2	-3.37	-5.64		AA'a-AA'c	0.48	0.64	
AA'a		5.9	5.8	2.1	2.1	2.7	2.7	11.1/11.1	8.3/8.3	-3.25	-5.74		AA'c-AA'a	0.71	0.43	

S5: Bader Charge Analysis

The Cu and Ru adatoms adsorbed on the (110) surface of ϵ -TaN are oxidized while those adsorbed on the (111) and (100) surfaces are partially reduced. To understand this behaviour, we performed Bader charge analysis and compared the charges of the surface atoms on a bare low-index surfaces with those when Cu/Ru adatoms are adsorbed at the A site on the respective surfaces in Figure S7. Comparing the charges on the bare surfaces (the top value on each atom) we clearly find that the (110) surface has the most oxidized Ta atoms and the most reduced N atoms. The average valence charge of Ta atoms on the (110) surface is 3.2, whereas this value is increased to 3.6 and 3.45 on the (111) and (100) surfaces. On the other hand the average valence charge of N atoms on the (110) surface is 6.3, which increases to 6.46 and 6.45 on the (111) and (100) surfaces, respectively. Therefore, when the Cu/Ru atoms are adsorbed on the (110) surface, the already oxidized S type Ta atoms gain electrons from them. The N atoms also gain electronic charge from the Cu adatom but not from Ru. This could be because of the larger electron affinity value of Cu (1.235) than Ru (1.046).

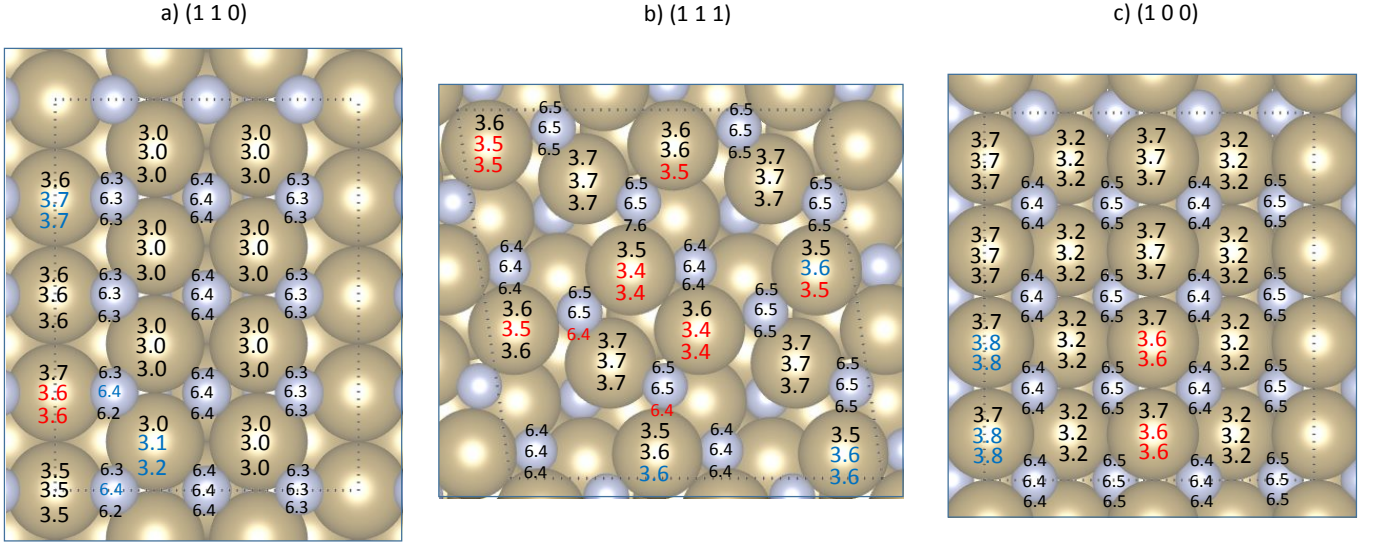


Figure S7: Bader charges of surface atoms on the low index surfaces of ϵ -TaN. There are three numbers listed for each surface atom. The number at the top is for the bare surfaces and the number in the middle and bottom is for the same surface where a Cu and Ru atom is adsorbed at the A site, respectively. Numbers in red indicate a decreased charge compared to the bare surface, numbers in blue indicate an increased charge.

On the (111) surface, clearly the surface S' type Ta atoms bound to Cu are further oxidized. This is probably due to their under coordination with N atoms as compared to the (110) surface. A similar observation is also made in the case of the (100) surface. However the charge transfer is smaller on the (100) surface as compared to the (111) and (100) surfaces. Moreover, on the (111) surface the charge transfer seems to be de-localized as compared to the (110) and (100) surfaces. There is also a high degree of corrugations and irregularities on the (111) surface as compared to the other two surfaces.

The surface charges on the doped surfaces compared to the bare surface show that doping causes the surface to become even more oxidised. Ru in RuA is the more oxidised than in RuB, indicating why RuA might be more reactive, but why RuB is more energetically stable. See Figure S8.

Comparing charges on 2x4 and 1x4 supercells shows that the electronic effect of doping is localised to those N and Ta atoms in direct vicinity of Ru. See Figure S9.

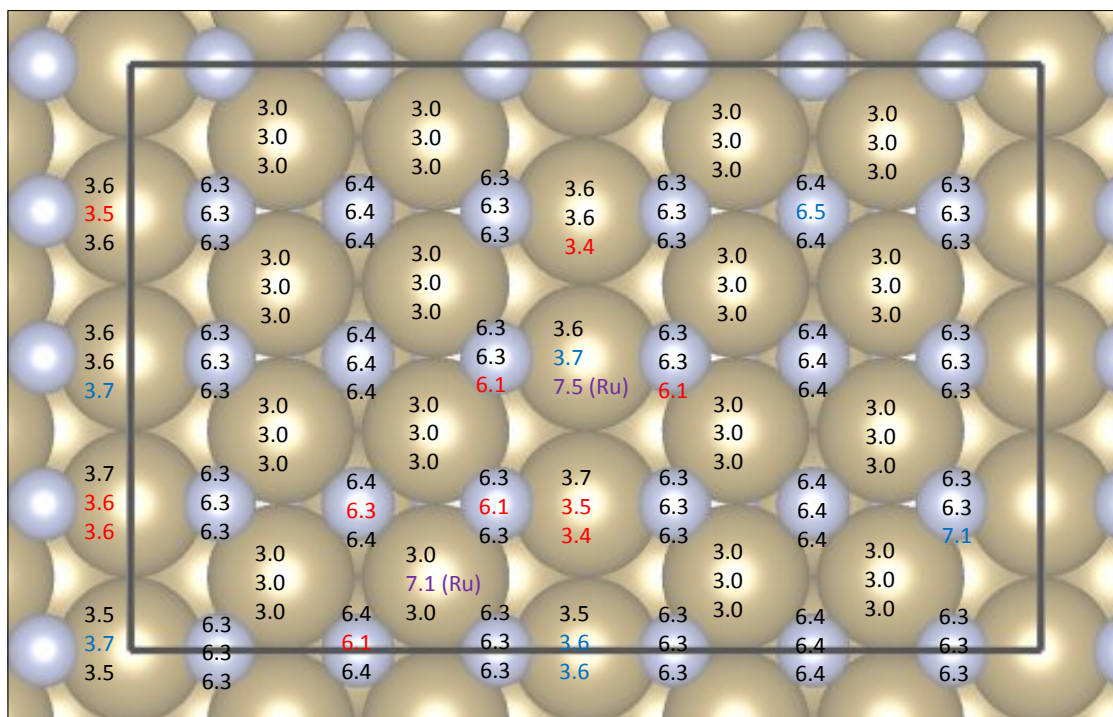


Figure S8: Bader charges of the surface atoms on the 2x4 supercell. The number at the top is for the bare surface, the second number is for RuA surface and the bottom number is for RuB surface. Charges of respective Ru atoms are shown in purple and labeled Ru. Numbers in red indicate a decreased charge compared to the bare surface, numbers in blue indicate an increased charge.

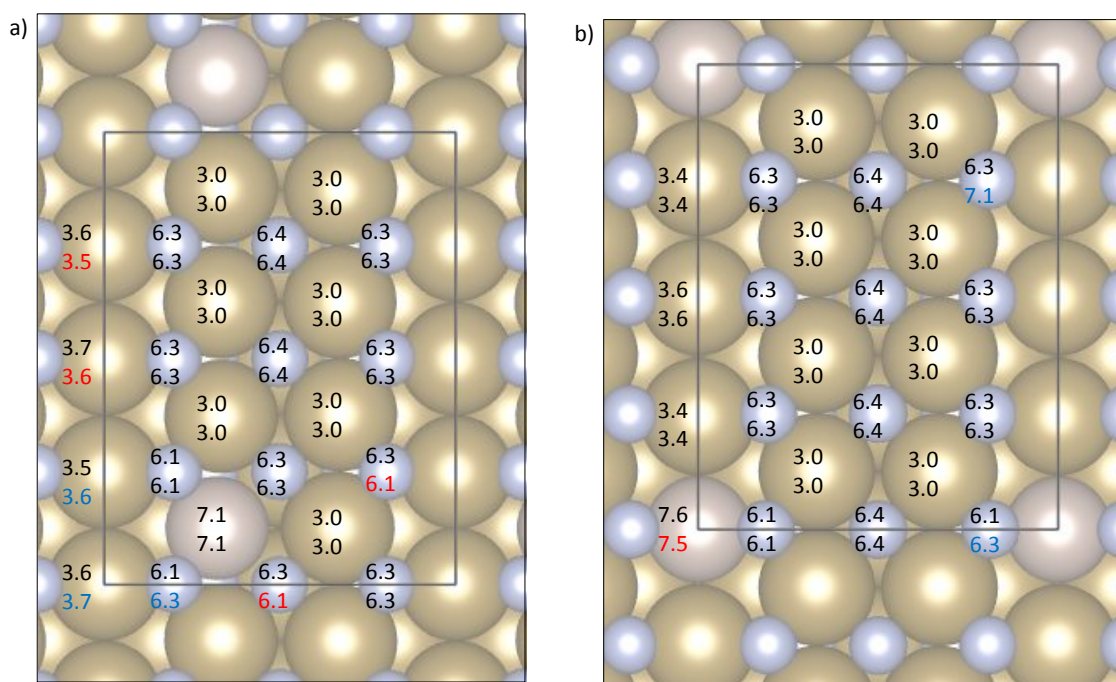


Figure S9: Bader charges of the surface atoms on the a) RuA and b) RuB 1x4 supercells. The number at the top is the charge on the 1x4 surface, the number at the bottom is the charge on the 2x4 surface. Red indicates the charge on the 2x4 surface is lower than on the 1x4 surface, blue indicated an increased charge.

S6: Density of States

From Bader charge partitioning analysis, we found that the Cu/Ru adatoms were oxidized on the (110) surface while they were reduced on the (111) and (100) surfaces. To understand this better, we compared the partial DOS of the adsorbed Cu/Ru atoms as shown in Figure S10. The total DOS plots of the bare surfaces are given in the first row and the PDOS plots of Cu and Ru adatoms at the most favourable site on these surfaces are shown in the second and third rows, respectively. From the second row in the case of (1 1 0) surface, we clearly find significant DOS of Cu in the conduction band separated from the valence band by a gap of approximately 1.5 eV which indicates oxidation. Whereas, on the (111) and (100) surfaces we do not find significant DOS beyond the fermi level which indicates a reduced Cu adatom. Similar to the copper case, the Ru adatom at the (1 1 0) surface has significant DOS beyond the fermi level indicating oxidation, however, its DOS at fermi level is non zero which is in contrast with PDOS of Cu. PDOS plots of Ru on the (111) and (100) surfaces have a non zero DOS at the fermi level which also extends into the conduction band suggesting a metallic nature.

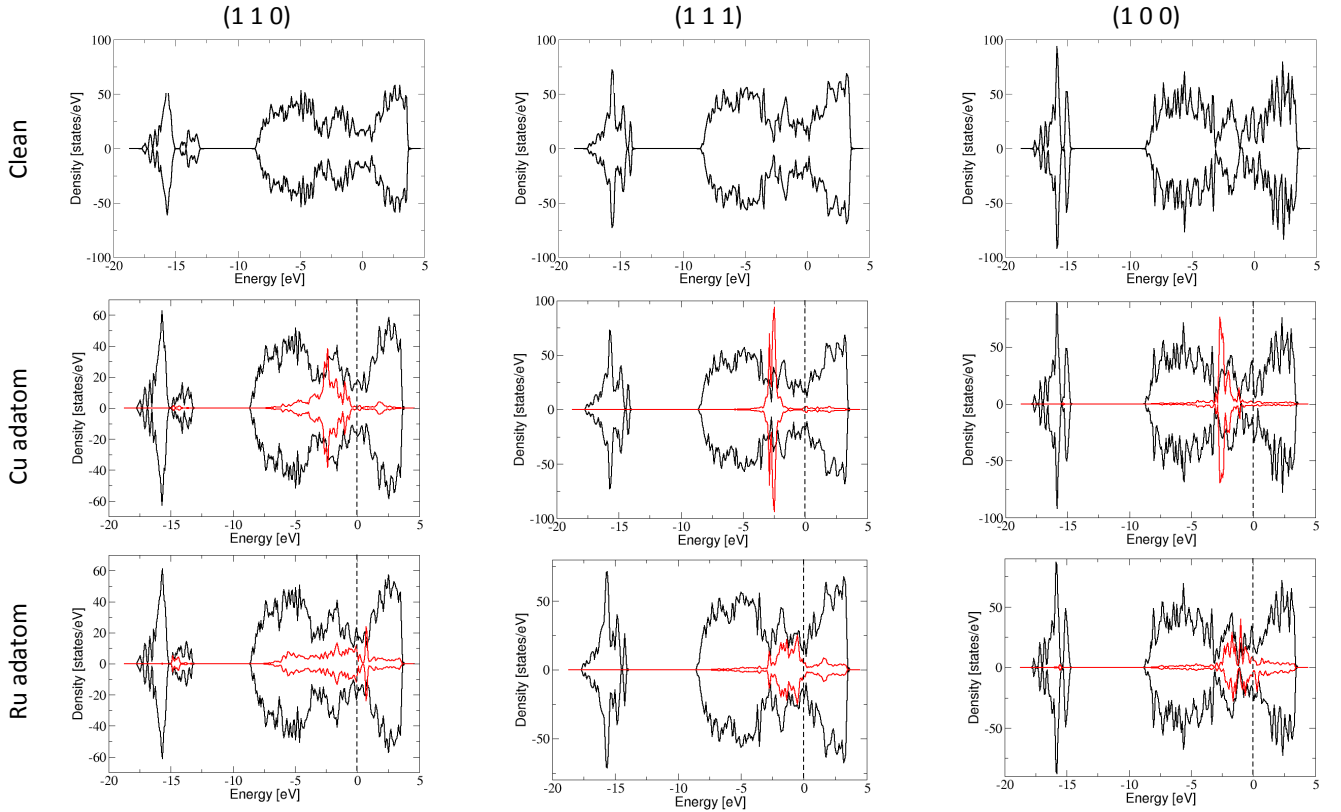


Figure S10: Total DOS of the bare TaN surfaces, total DOS of Cu/Ru adsorbed at the most favourable site on the TaN surfaces, and PDOS of Cu/Ru adatoms. The PDOS plots of Cu and Ru are shown in red and are scaled by a factor of 10.

S7: Cu on Ru passivated TaN

Several Ru atoms are first adsorbed on the TaN (1 1 0) surface as shown in Figure S11a-f so as to obtain a model of the saturated surface and the corresponding binding energies per adsorbed Ru atom are plotted in Figure S11g. From the geometries in Figure S11a-c, where 3-9 Ru atoms are adsorbed, we find that the adatoms preferentially bind at sites A, A' and B on the TaN (1 1 0) surface. As the coverage increases to 12 Ru/supercell, the adatoms at site B are displaced to the atop N site adjacent to B and initiate the formation of a closely packed structure. At a coverage of 16 Ru per supercell, where one monolayer of Ru is coated on the surface, we find a hexagonal packing of the Ru atoms. Two monolayers of Ru coverage is obtained at 32 Ru per supercell as shown in Figure S11f where a fully formed HCP surface of Ru is visible. From Figure S11g we observe that the binding energy per Ru increases up to 6 Ru adsorption and then decreases with additional Ru atoms as they begin to associate on the surface. This trend will continue until the binding energy reaches the cohesive energy of bulk Ru (6.8 eV). At 3 adatom adsorption the Ru adatoms are oxidized, similar to the 1 and 2 adatom cases discussed earlier, with valence charges in the range of 7.5 - 7.7. This range increases to 7.6 - 7.8 at 6 Ru adsorption and 7.7 - 7.9 at 9 and 12 Ru adsorptions. At 1 ML coverage, the Ru adatoms are less oxidized, with valence charges in the range of 7.8 - 8.1. At 2 ML coverage, the bottom layer of Ru atoms are slightly oxidized with the valence charge in the range 7.7 to 7.9 while the top layer is metallic with the valence charge between 8.0 and 8.1.

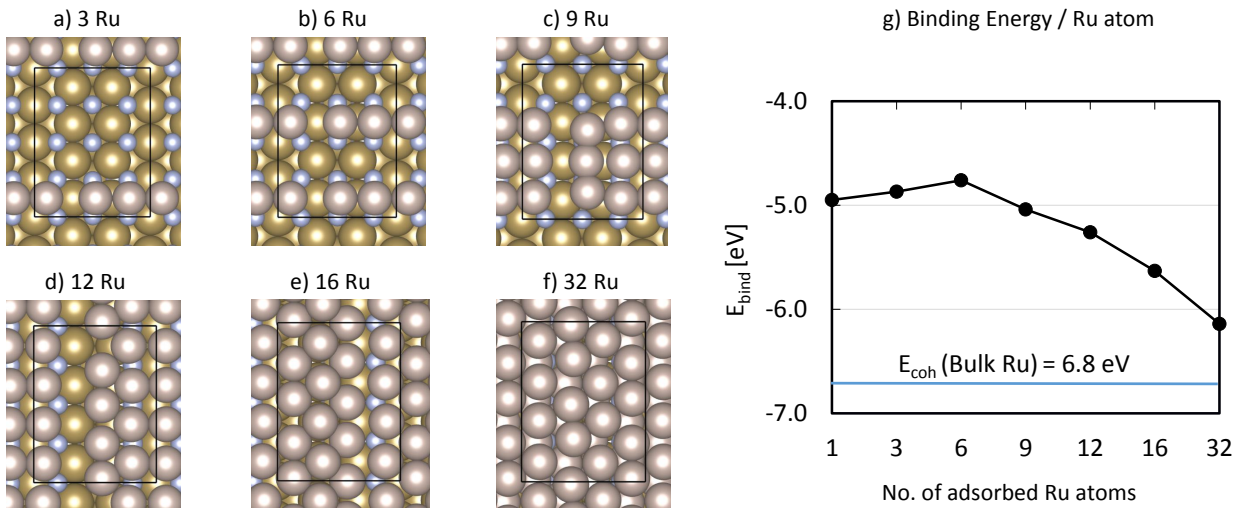


Figure S11: Panels a)-f) show minimum geometries representing Ru passivated TaN (1 1 0) surface. The graph in panel g) shows the binding energy per Ru atom adsorbed on the TaN (1 1 0) surface. The blue line indicates the cohesive energy of Ru in bulk state. The Ta, N and Ru atoms are shown in ochre, light blue and brown, respectively.

Three stable binding sites (A, B and C) are found for a Cu adatom at the 1 ML of Ru passivated TaN(1 1 0) surface (Figure 6 of main text) and the corresponding binding energies are listed in Table S4. Site A is a wide 3 fold site above a sub-surface N atom, site B is another wide 3 fold site above a sub-surface Ta atom and site C is a two fold site. The binding energies are within the range of -3.2 eV to -3.5 eV where the strongest binding is seen at site B and the weakest binding at site A. Moreover the binding energies are also moderately lower than on the bare (1 1 0) surface suggesting the favourable aspect of Ru passivation. We did not find significant changes in the valence charge of the adsorbed Cu atom which indicates that there is no significant electron transfer between the Cu adatom and the Ru layer and Cu remains metallic. On the 1 ML passivated surface, the geometries at A_{exch} and C_{exch} have the highest binding energies, whereas the geometry at B_{exch} has comparable binding energy to that of the on-surface adsorption. The forward activation energies for the exchange diffusion are significantly larger than for the reverse process and also considerable larger than that of the on-surface diffusion.

On the 2 ML of Ru passivated TaN(1 1 0) surface, four unique stable binding sites for 1 Cu adsorption (A, B, C and D) are found as shown in Figure 6c and the corresponding binding energies are listed in Table S4. The binding energies are in the range of -3.13 eV to -3.44 eV, which are comparable to the 1 ML Ru passivated surface. The two fold Ru coordinated site A is found to be the most favourable followed by B, C and D, each of which are three fold coordinated by Ru atoms. Similar to the 1 ML case, there is no significant charge transfer between the Cu and Ru atoms. As the next step, adsorption of 2 Cu is investigated where the first Cu is placed at the most favourable binding site (site B) and the second Cu is placed at sites A, C, D, B' and A' (we use combined site notation BA, BC, BD, BB' and BA' to represent the 2 atom adsorption site). From Table S4 we find that the binding energies per Cu adatom are in the range of -3.48 eV to -3.60 eV. Compared to the 1 Cu adsorption case, we find that the binding energies have decreased slightly, probably due to the additional Cu-Cu interaction and associated surface rearrangements. We found the geometry at site BB' to be the most favourable where the Cu atoms are at a distance of 2.47 Å.

Table S4: Binding energies and activation energies for the diffusion of Cu adatoms on 1 and 2 ML of Ru passivated TaN (1 1 0) surfaces. A '-' for the E_{bind} indicates that the respective geometry is found to be unstable and a '-' for $E_{\text{activation}}$ indicates that we could not find a transition state connecting the minima.

Adatoms	Sites	Q(Cu)	E _{bind} [eV]	d(Cu-Cu) [Å]	Pathway	E _{activation} [eV]	
						Forward	Reverse
1 ML Ru							
1 Cu	A (3 fold atop N)	10.9	-3.24		A-B	0.01	0.21
	B (3 fold atop Ta)	11.0	-3.44		B-C	0.45	0.37
	C (2 fold)	10.9	-3.35				
	A _{exch}	10.8	-2.51		A-A _{exch}	0.84	0.11
	B _{exch}	10.8	-3.12		B-B _{exch}	0.72	0.41
	C _{exch}	11.0	-2.71		C-C _{exch}	1.03	0.38
2 Cu	BB'	11.0/11.0	-3.60	2.5			
	BA	11.0/11.0	-3.48	2.6	BB' - BA	0.44	0.20
	BC	11.0/10.9	-3.49	2.9	BB' - BC	0.48	0.24
	BB''	11.0/10.9	-3.52	5.2	BB' - BB''	0.35	0.18
2 ML Ru							
1 Cu	A (2 fold)	11.0	-3.44		A-B	0.46	0.44
	B (3 fold wide)	11.0	-3.42		A-C	-	-
	C (3 fold hcp)	10.9	-3.18		A-D	-	-
	D (3 fold hollow)	10.9	-3.13				
	A _{exch}	11.0	-2.41		A-A _{exch}	1.93	0.89
	B _{exch}	11.0	-2.07		B-B _{exch}	2.19	0.83
	C _{exch}	11.0	-2.17		C-C _{exch}	1.39	0.38
	D _{exch}	11.0	-2.22		D-D _{exch}	-	-
2 Cu	AA'	11.0/10.9	-3.43	2.7			
	AB	11.0/11.0	-3.43	2.5	AA' - AB	0.20	0.19
	AC	11.0/10.9	-3.35	2.4			
	AB'	10.9/11.0	-3.31	4.8	AA' - AB'	0.30	0.06
	AC'	11.0/10.9	-3.30	4.6	AA' - AC'	-	-

S8: Cu on Ru-doped TaN

The activation energies for each migration pathway are shown in Table S5. For reference the binding energies and charges that are presented in the main text are included again. Further, the geometries of all stable adsorption sites can be found in Fig. S13, S14, S15 and ??.

Table S5: Binding Energies of Cu on Ru-doped TaN(1 1 0), as well as the activation energies for facile diffusion on the surface. The forward direction for activation energies indicates Cu moving away from Ru, while the reverse indicates Cu moving towards Ru. $Q(\text{Cu})$ is the charge on the Cu atom adsorbed to a doped surface, where there are two adatoms the charges are separated by a " / "

No.	Cu	Ru doping site	Cu adsorption site	E_{bind} [eV]			$Q(\text{Cu})$	Migration Pathway	$E_{\text{activation}}$ [eV]	
				doped 1x4	doped 2x4	bare 2x4			Forward	Reverse
1	Cu	RuB	A	-2.88	-2.92	-2.80	10.5	A-A'	0.80	0.73
			B	-2.02	-2.09	-2.02	10.5	A-A''	0.40	0.38
			C	-1.88	-1.94	-1.90	10.6	A-B	1.42	0.56
			D	-2.56	-2.63	-2.13	10.4	B-B'	0.14	0.10
			E		-2.14		10.5			
2	Cu	RuA	AA''c		-3.12	-3.03	10.5/10.6	AA'c-AA'a	0.70	0.66
			AA''a		-3.34	-2.79	10.5/10.5			
			AB		-3.21	-2.42	10.6/10.5			
			AC				10.6/10.5			
			AD		-3.05	-2.42	10.5/10.4			
	Cu	RuB	AA''c		-3.03	-3.03	10.5/10.6	AA'c-AA'a	0.60	0.72
			AA''a		-2.88	-2.79	10.5/10.5			
			AB		-2.51	-2.42	10.5/10.5	-		

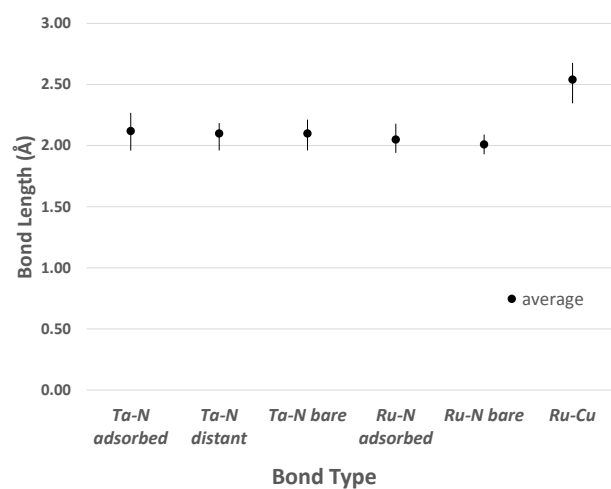


Figure S12: Average, maximum and minimum bond lengths measured. These values are based on measurements from Cu adsorption on both RuA and RuB surfaces. "Ta-N adsorbed" are bonds where N is directly bound to Cu at an adsorption site, "Ta-N distant" are bonds at an equivalent site on the surface away from the adsorption site and "Ta-N bare" was measured on a clean, doped surface. Similarly, "Ru-N adsorbed" are measured on a doped surface where Cu atoms have adsorbed and "Ru-N bare" was measured on the clean, doped surface.

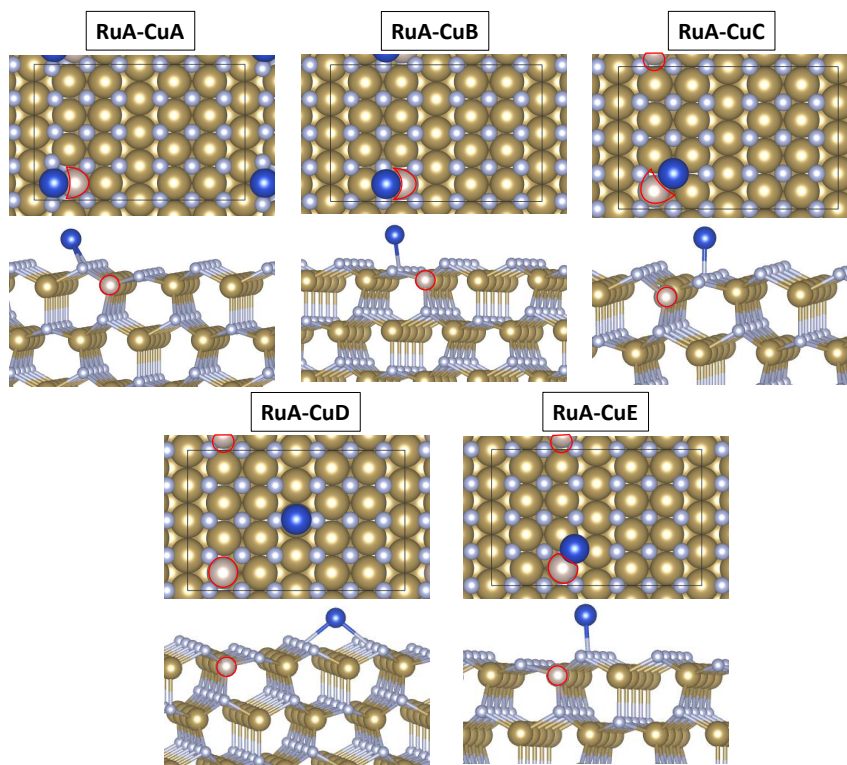


Figure S13: The adsorption geometries of 1 Cu atom on RuA-doped TaN(1 1 0). The Ta, N, Ru and Cu atoms are shown in ochre, light blue, brown and blue, respectively. Ru atoms are highlighted with a red border.

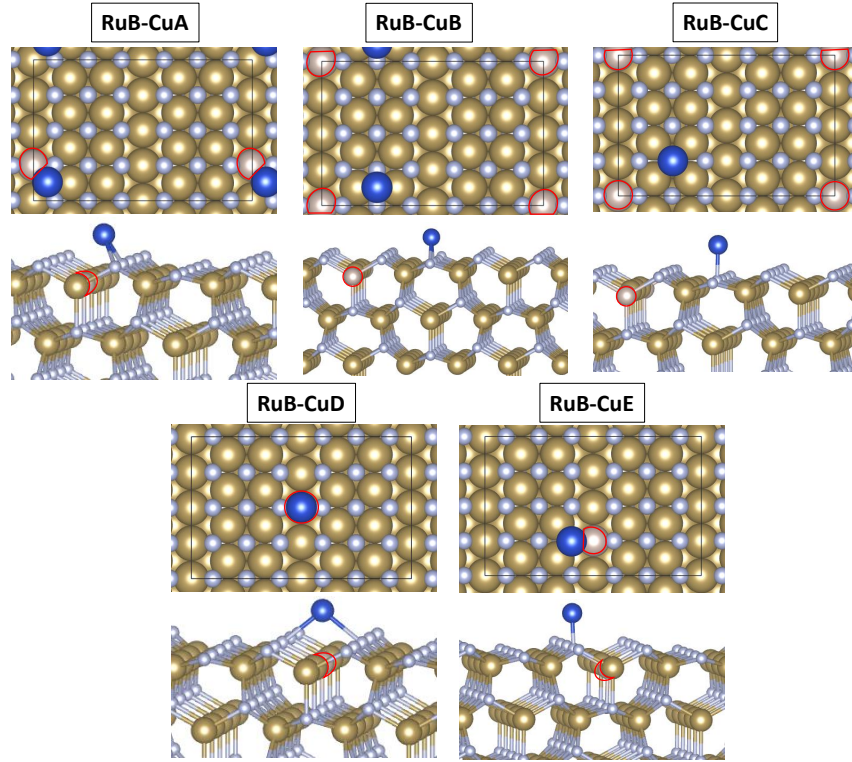


Figure S14: The adsorption geometries of 1 Cu atom on RuB-doped TaN(1 1 0). The Ta, N, Ru and Cu atoms are shown in ochre, light blue, brown and blue, respectively. Ru atoms are highlighted with a red border.

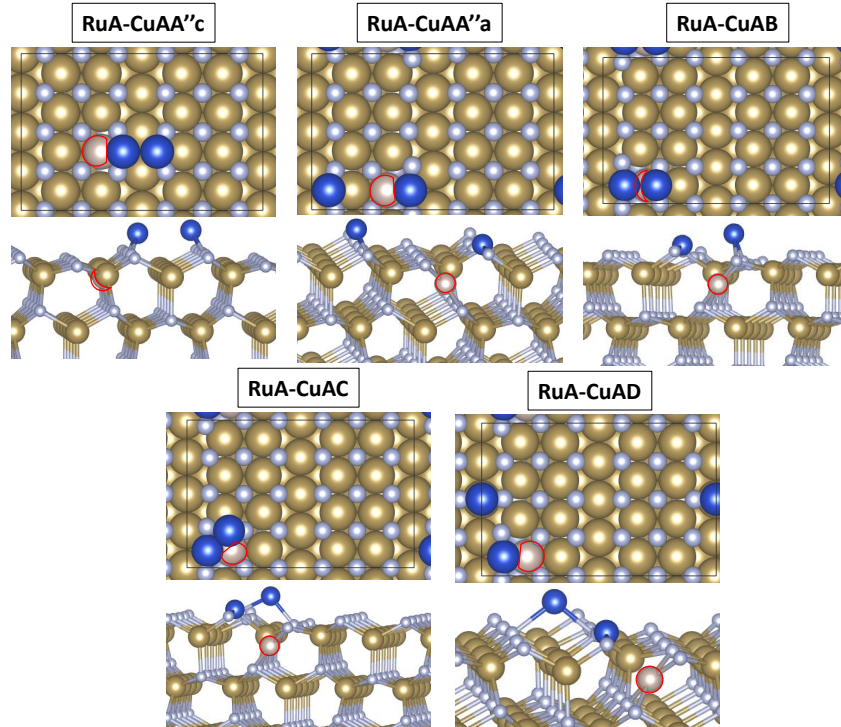


Figure S15: The adsorption geometries of 2 Cu atoms on RuA-doped TaN(1 1 0). The Ta, N, Ru and Cu atoms are shown in ochre, light blue, brown and blue, respectively. Ru atoms are highlighted with a red border.

References

[Frisk(1998)] K. Frisk, *J. Alloy. Compd.*, 1998, **278**, 216–226.